Public reporting burden for this collection of information is estimated to average 1 hour per response including the time ~~~~~~~~~~ and
maintaining the data needed, and completing and reviewing the collection of information. Send comments regarding tl ~~~~~~~~~ ion,
including suggestions for reducing this burden, to Washington Headquarters Services, Directorate for Information Operatic ~~~~~~~ VA
22202-4302, and to the Office of Management and Budget, Paperwork Reduction Project (0704-0188), Washington, DC 2C ~~~~~~

1. AGENCY USE ONLY (Leave blank)	2. REPORT DATE 21 October 2004	3. REPORT TYPE AND DATES COVERED Final Report

4. TITLE AND SUBTITLE High Throughput Synthesis of Terahertz Quantum Cascade Lasers	5. FUNDING NUMBERS FA9550-04-C-0018
6. AUTHOR(S) Kurt J. Linden, Ph.D.	

7. PERFORMING ORGANIZATION NAME(S) AND ADDRESS(ES) Spire Corporation One Patriots Park Bedford, MA 01730	8. PERFORMING ORGANIZATION REPORT NUMBER 60454

9. SPONSORING/MONITORING AGENCY NAME(S) AND ADDRESS(ES AFOSR/NE 4015 Wilson Blvd. Room 713 Arlington, VA 22203-1954	10. SPONSORING/MONITORING AGENCY REPORT NUMBER

11. SUPPLEMENTARY NOTES

12a. DISTRIBUTION/AVAILABILITY STATEMENT Distribution Statement A: unlimited	12b. DISTRIBUTION CODE

13. ABSTRACT (Maximum 200 words)

This Phase I STTR program (Topic #AF03T024) was aimed at the design and synthesis of an AlGaAs/ GaAs-based epitaxial layer structure for terahertz quantum cascade lasers (THz QC lasers) that can be grown by metalorganic chemical vapor deposition (MOCVD). The program succeeded in growing two different THz QC laser structures by MOCVD. The wafer growths of these 10 micron thick epitaxial structures by MOCVD required 5 hours of growth time, compared to one day for the competing MBE growth technology. This was the first successful demonstration of an MOCVD-grown terahertz laser structure. Verification of the epitaxial layer parameters was carried out by scanning transmission electron microscopy, verifying conformance to design specifications within 0.16%. A highly efficient terahertz laser design, consisting of a metal-semiconductor-metal (MSM), planar waveguide structure, was theoretically analyzed and found to be the best design for low threshold current and high laser operating temperature. Phase I demonstrated that it is possible to grow high-quality THz QC laser material by the production-amenable, high wafer capacity MOCVD technology, while Phase II will utilize this design for laser fabrication.

14. SUBJECT TERMS Phase I STTR program Terahertz laser, quantum cascade, MOCVD growth, agent detection, Wi-Fi			15. NUMBER OF PAGES 18
			16. PRICE CODE

17. SECURITY CLASSIFICATION OF REPORT Unclassified	18. SECURITY CLASSIFICATION OF THIS PAGE Unclassified	19. SECURITY CLASSIFICATION OF ABSTRACT Unclassified	20. LIMITATION OF ABSTRACT Unclassified

nsn 7540-01-280-5500

Standard Form 298 (Rev. 2-89)
Prescribed by ANSI Sts 239-18

i

Final Report:

HIGH THROUGHPUT SYNTHESIS OF TERAHERTZ QUANTUM CASCADE LASERS

Contract Period

22 December 2003 through 21 September 2004

Reporting Period:

22 December 2003 through 21 September 2004

Submitted under:

Contract No. FA9550-04-C-0018

Submitted to:

AFOSR/NE

Dr. Gernot Pomrenke

4015 Wilson Blvd., Room 713

Arlington, VA 22203-1954

Prepared by:

Kurt J. Linden, Ph.D.

Submitted by:

Spire Corporation

One Patriots Park

Bedford, MA 01730-2396

TABLE OF CONTENTS

LIST OF FIGURES

LIST OF TABLES

1. INTRODUCTION

This Phase I STTR program was aimed at the design and synthesis of an AlGaAs/GaAs-based epitaxial layer structure for terahertz quantum cascade lasers (THz QC lasers) that can be grown by metalorganic chemical vapor deposition (MOCVD). The program succeeded in growing two different THz QC laser structures by MOCVD, one designed for 3 THz emission, and one designed for 4 THz emission. The wafer growths of these 10 micron thick epitaxial structures by MOCVD required 5 hours of growth time, compared to a period of approximately one day for the competing, currently-used MBE epitaxial growth technology. This was the first demonstration of an MOCVD-grown terahertz laser structure. Verification of the epitaxial layer parameters were carried out by carrier concentration profiling, photoluminescence, and scanning transmission electron microscopy (STEM) analysis. Each of these analyses verified conformance to design specifications, and epitaxial layer thickness consistency and run-to-run reproducibility over a 3-month period was verified to within 0.16%. A highly efficient terahertz laser design, consisting of a metal-semiconductor-metal (MSM), planar waveguide structure, was theoretically analyzed and found to be the best design for low threshold current and high laser operating temperature. Phase I demonstrated that it is possible to grow high-quality THz QC laser material by the production-amenable, high wafer capacity MOCVD technology. Phase II will utilize this new MSM device design and further develop this epitaxial growth capability to demonstrate operational QCL devices as obtained from a high-volume semiconductor fabrication foundry.

The work on this SBIR project was carried out at Spire, the University of Illinois, and Bandwidth Semiconductor, subsidiary of Spire. The University of Illinois group, consisting of Prof. Shun Lien Chuang and graduate student Maytee Lerttamrab, carried out epitaxial structure calculations and laser device modeling. The Bandwidth Semiconductor group working on the epitaxial growth and characterization of the quantum cascade laser wafers consisted of Victor Haven and Tri Ta. Kurt Linden was the principal investigator on this project.

2. WORK CARRIED OUT DURING THE CONTRACT PERIOD

2.1 Terahertz Cascade Laser Epitaxial Layer Design Methodology

Theoretical studies of terahertz quantum cascade laser designs were carried out by subcontractor University of Illinois Urbana Champaign (UIUC). The UIUC group developed a temperature dependent electronic band structure model for the GaAs/Al(0.15)Ga(0.85)As material system. For a given structure, the Schrödinger equation and Poisson equation were self-consistently solved using the finite difference method for the wave functions and energy levels of the structure (Ref. 1). The wave functions were then used to calculate the optical dipole moments and later the material gain. Since the THz transition to be investigated was an intersubband process, the material gain spectra assumed a Lorentzian line shape.

In order to double-check the UIUC simulation, a comparison was made between the UIUC results and the published work from MIT on 4-coupled quantum wells (Ref. 2) as shown in Figure 1.

The squared wave functions in the UIUC simulation, Figure 1(a), seem to match very well with MIT's result in Figure 1(b). The simulation shows a 3.53-THz energy transition (E_{54}) corresponding to 14.6 meV, which is close to MIT's result of 13.9 meV for an applied electric field of 12.2 kV/cm at 4 K.
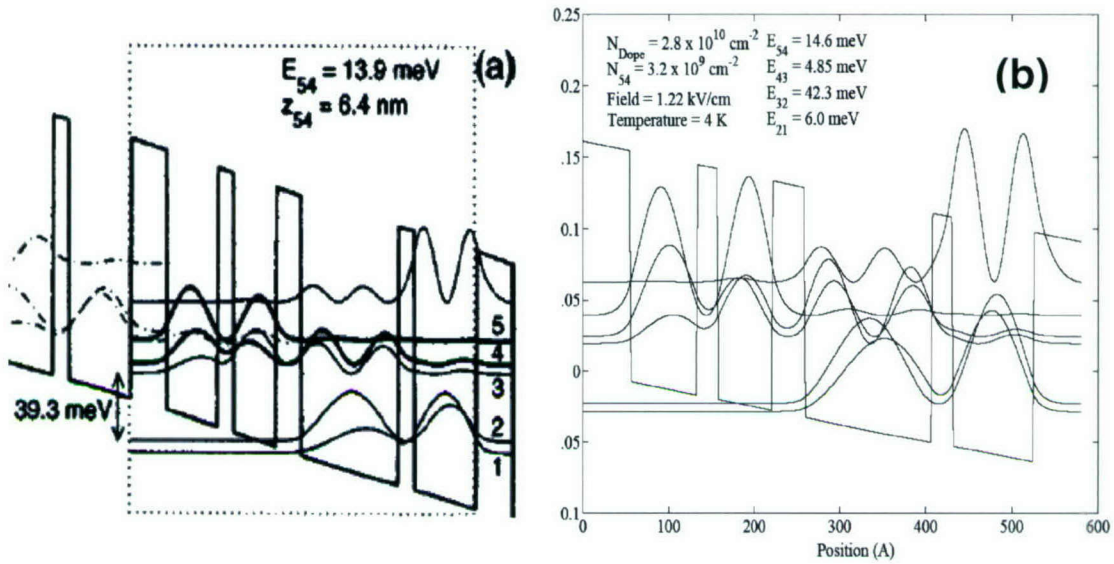
Figure 1 (a) MIT's 4-coupled quantum-well structure (Ref. 2). (b) UIUC's simulation of MIT's 4-coupled quantum-well structure.

The initial design of a THz QCL structure was then undertaken. The initial goal was to design a laser with a lasing frequency of 4 THz or a wavelength of 75 μm. Since the lasing frequency of MIT's 4-coupled quantum-well structure is around 3.4 THz, by modifying this structure it was possible to extend the lasing frequency of ~ 4 THz. The design rules used are described here. The transition from level 5 to 4, E_{54}, is fixed to near 16.3 meV, which will generate ~ 4 THz radiation. In order to achieve population inversion between level 5 and 4, it is necessary to remove electrons from level 4 to level 3 as fast as possible by keeping these two levels anticrossed. By utilizing longitudinal-optical (L-O) phonon, one can depopulate electrons in level 3 into levels 2, and 1. Electrons in levels 2 and 1 are then injected into level 5 of the next module of the cascade structure. Some of the parameters used in the simulation are taken from Ref. 3. The structure of this design is shown in Fig. 2(a) with the following dimensions in Å starting with the injector barrier on the left, 54/76/22/70/38/148/24/94, where the 148-Å well is doped with sheet carrier density of 2.8×10^{16} cm^{-2}. The calculated material gain spectrum in Figure 2(b) shows a peak position near 4 THz.

The same design methodology was used to generate a basic epitaxial layer design for a 3 THz quantum cascade laser, thus providing the basic designs for both the 3 THz and 4 THz quantum cascade laser structures based on the MQW design approach. Both of these epitaxial structures were then grown by the MOCVD growth technology. The basic epitaxial layer designs for these two structures are summarized in the following section.

2.2   Terahertz Cascade Laser, 3 THz and 4 Thz Epitaxial Layer Design Results

This section of the final report summarizes epitaxial layer details of both the 3 THz and 4 THz quantum cascade laser designs generated by the UIUC group. Details of the 3 THz cascade laser design are shown in Table 1.

$N_{Dope} = 2.8 \times 10^{10}$ cm^{-2} $E_{54} = 16.3$ meV
$N_{54} = 3.2 \times 10^9$ cm^{-2} $E_{43} = 5.35$ meV
Field = 1.33 kV/cm $E_{32} = 42.5$ meV
Temperature = 4 K $E_{21} = 6.33$ meV

(a)

Peak position ~ 4 THz

(b)
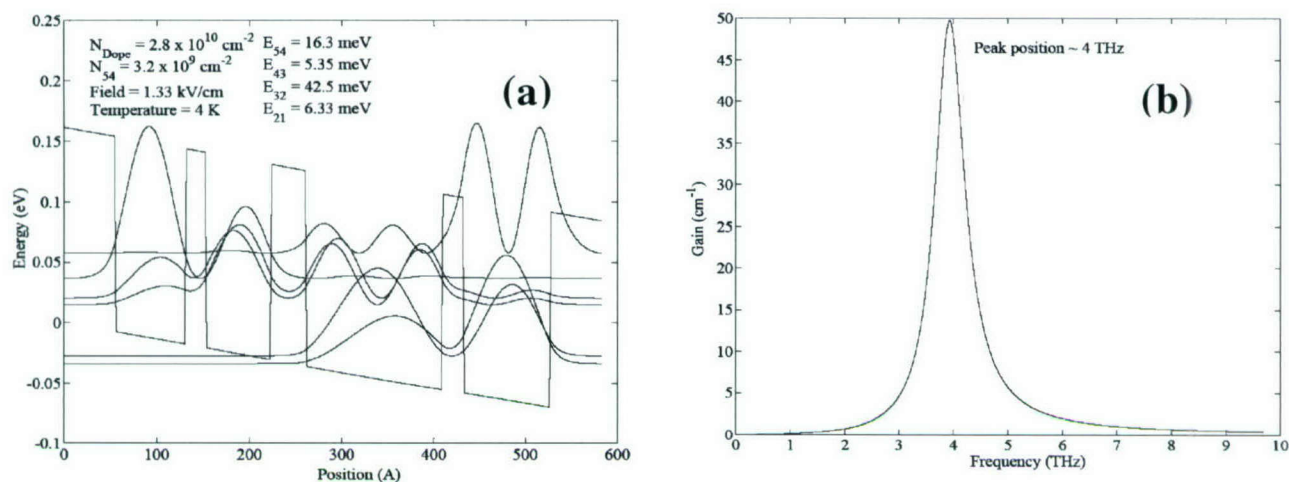
Figure 2   (a) UIUC's simulation of the band structure, wave functions, and energy levels for a 4-well THz QCL. The 4-well structure is outlined beginning with the left injection barrier, the layer thickness in Å are 54/76/22/70/38/148/24/94, where the 148-Å well is doped with sheet carrier density of 2.8×10^{10} cm^{-2}. (b) The material gain peak is close to 4 THz.

Table 1   Epitaxial layer design of the 3 THz quantum cascade laser structure as generated by UIUC.

Layer (3 THz Design)	Material	t (Å)	Doping	Total thickness, t
Cladding	GaAs	600	n=5x10^{18} cm^{-3}	↑
↑	GaAs	94	undoped	
	Al$_{0.15}$Ga$_{0.85}$As	34	undoped	
572 Å /period	GaAs	160	n=2x10^{16} cm^{-3}	Total thickness, first
	Al$_{0.15}$Ga$_{0.85}$As	44	undoped	AlGaAs to top of wafer
(150 times on first growth)	GaAs	70	undoped	surface = 8.64 microns
	Al$_{0.15}$Ga$_{0.85}$As	24	undoped	
	GaAs	90	undoped	
↓	Al$_{0.15}$Ga$_{0.85}$As	56	undoped	↓
Cladding	GaAs	8000	n=3x10^{18} cm^{-3}	
Semi-Insulating Substrate	GaAs		undoped	Substrate

The structure was selected to contain 150 periods, each of which had a thickness of 572 angstroms. This resulted in a total epitaxial layer thickness of 86,400 angstroms or 8.64 microns. Only the central GaAs epitaxial layer of each period is lightly doped (2×10^6 cm^{-3}).

Details of the 4 THz quantum cascade laser design are shown in Table 2.

3

Table 2 Epitaxial layer design of the 4 THz quantum cascade laser structure as generated by UIUC.

| Layer (4 THz Design)	Material	t (Å)	Doping	Total thickness, t
Cladding (run M1-1280)	GaAs	600	$n=5 \times 10^{18}$ cm^{-3}	↑
↑	GaAs	94	undoped	
	Al$_{0.15}$Ga$_{0.85}$As	24	undoped	
526 Å /period	GaAs	148	$n=2.6 \times 10^{16}$ cm^{-3}	Total thickness, first
	Al$_{0.15}$Ga$_{0.85}$As	38	undoped	AlGaAs to top of wafer
(150 times on first growth)	GaAs	70	undoped	surface = 7.95 microns
	Al$_{0.15}$Ga$_{0.85}$As	22	undoped	
	GaAs	76	undoped	
↓	Al$_{0.15}$Ga$_{0.85}$As	54	undoped	
Cladding	GaAs	8000	$n=3 \times 10^{18}$ cm^{-3}	
Semi-Insulating Substrate	GaAs		undoped	Substrate

This structure also has 150 periods, but here each of the periods had a thickness of 526 angstroms. This resulted in a total epitaxial layer thickness of 79,500 angstroms or 7.95 microns. Again, only the central GaAs epitaxial layer of each period was lightly doped (2×10^6 cm^{-3}).

2.3 Epitaxial Wafer Growth and Evaluation of the 3 Terahertz Laser Structure

The entire epitaxial structure consists of a semi-insulating substrate covered with a conducting GaAs layer, followed by 150 eight-layer groups of identical structure (total of 1,200 epitaxial layers), and topped off with a GaAs cladding layer. Such complex structures are extremely demanding on the epitaxial growth system controls and components, requiring over one thousand two hundred valve openings and closings and an equivalent number of mass-flow controller operations. All 8-layer groups must be identical to within a monolayer thickness throughout the entire structure. When grown by the competing and more-commonly-used molecular beam epitaxial (MBE) growth method, this type of structure imposes severe operating conditions on the system, required heavy wear and tear on the system shutters and requiring over approx. 24 hours of growth time. Since MOCVD growth is much faster than MBE growth, the former method has a significant advantage. In addition, the large volume capacity of Spire's MOCVD growth system (eight 3" diameter wafers or twenty one 2" diameter wafers per growth run) facilitates production of large quantities of uniform wafers in a relatively short time.

Prior to growth of the structure, the MOCVD system was calibrated by growing thick test layers of each of the two compositions, and then measuring the layer thicknesses to determine growth rates. Epitaxial growth of the 3 THz QC laser design (growth run number M1-1189) was successfully completed early in the Phase I program, and STEM analysis was carried out on portions of one of the several wafers produced in this growth run by Materials Analytical Services (MAS), Inc. of Raleigh, NC. The resulting STEM analysis of this wafer verified excellent conformance to design specifications. The design of this 3 THz structure is summarized in Table 1 above. The STEM cross-section photographs obtained from MAS are shown in the following figures. Figure 3 shows a cross-section of this structure with a scale factor of 600 nm as indicated in the lower right portion of the photograph. Each division of this scale corresponds to 60 nm (600 angstroms). The photograph shows 48 periods of the structure, with all layers clearly identifiable.
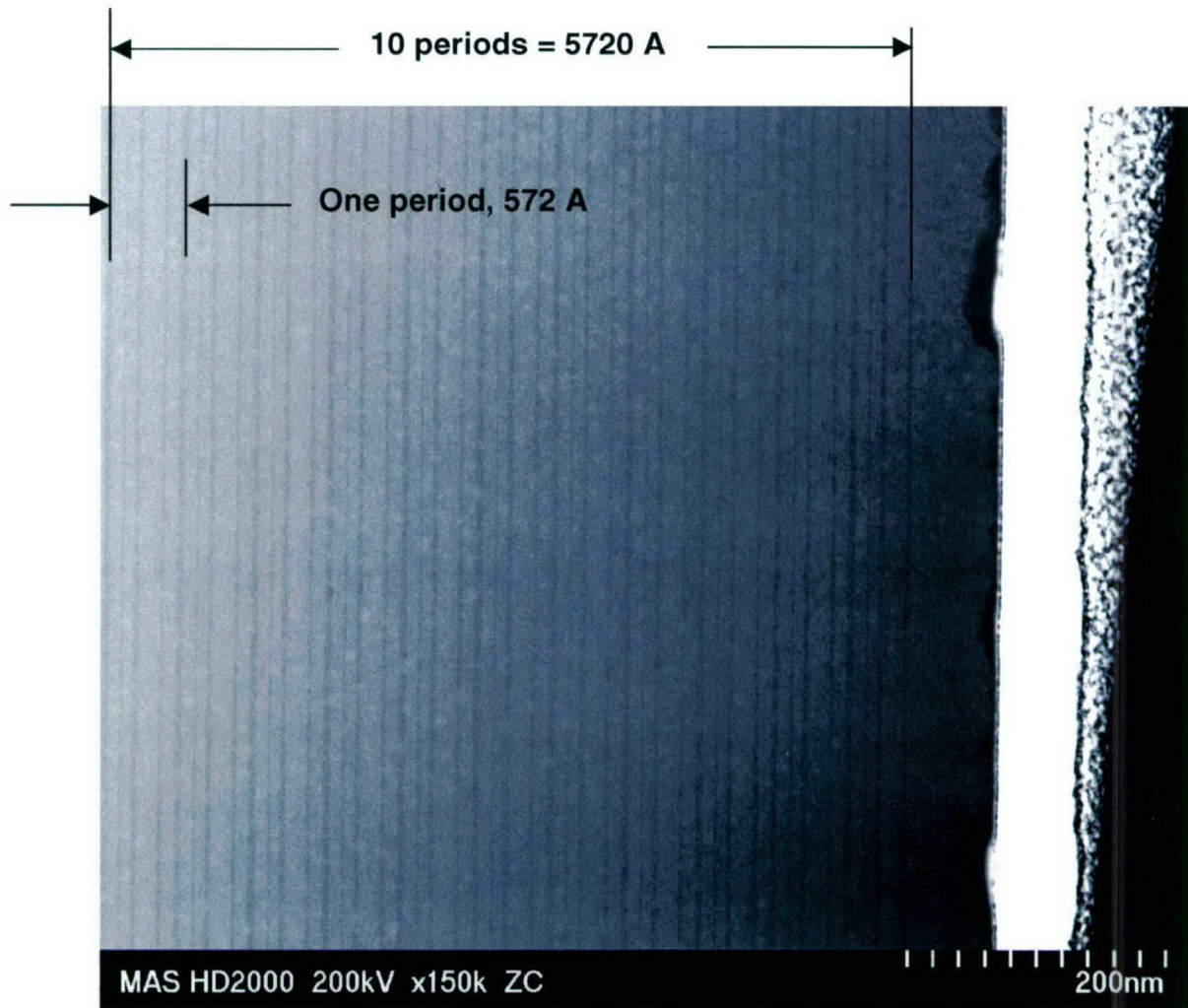
Top 48 periods

MAS HD2000 200kV x50.0k ZC   600nm
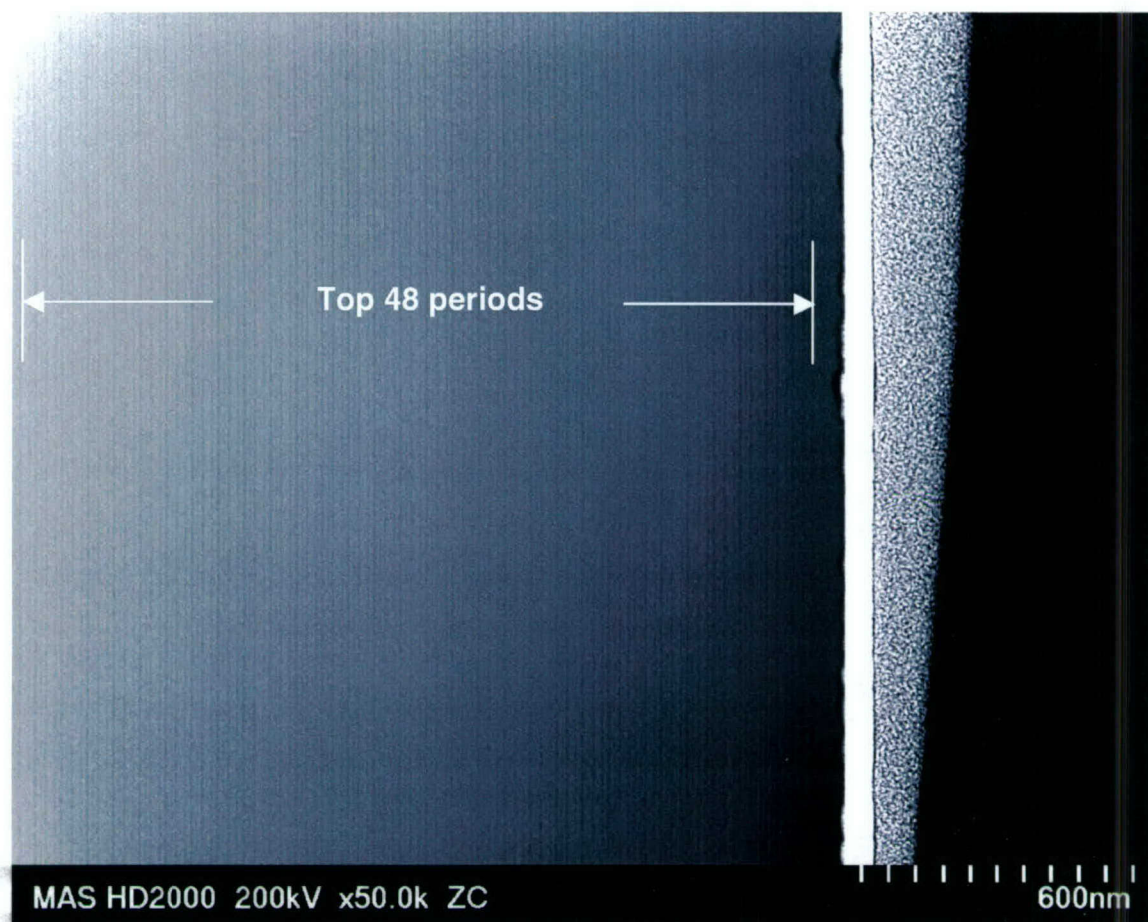
Figure 3 **STEM cross-section photograph of Wafer No. M1-1189, section m02. Dark bands are Al(0.15)Ga(0.85)As, and gray bands are GaAs. Surface of wafer is at right side of photograph. Magnification adjusted to show 48 periods of the cascade structure.**

A somewhat higher resolution STEM cross section photograph is shown in Figure 4, with a linear scale of 200 nm, showing 10 periods of the cascade structure. Here the layers are more readily identifiable, corresponding to the Table 1 design.

The highest magnification photograph taken for this sample, adjusted to provide a detailed cross-section of just one period of the structure, is shown in Figure 5.

These three different STEM cross-section magnifications illustrate the excellent thickness uniformity and thickness control achieved in this growth. The measured numbers indicated in Figure 3 are very close to the design thicknesses shown in Table 1 of this report. For example, visual observation of the 48 periods of layer groups shown in Figure 3 show excellent layer thickness uniformity, while the most detailed layer analysis shown in Figure 5 illustrates the outstanding layer thickness control to within a monolayer of atoms. Also, the transitions between the layers are very abrupt, probably monolayer abrupt. Such sharp interfaces were achieved by reducing the layer growth rate and increasing the hydrogen carrier gas flow to the point where residual source gas compositions are changed in a time short compared to the monolayer growth time.

5

10 periods = 5720 A

One period, 572 A

MAS HD2000 200kV x150k ZC

200nm

Figure 4 **STEM cross-section photograph of Wafer No. M1-1189, section m04. Dark bands are Al(0.15)Ga(0.85)As and gray areas are GaAs. Top of wafer is on the right.**
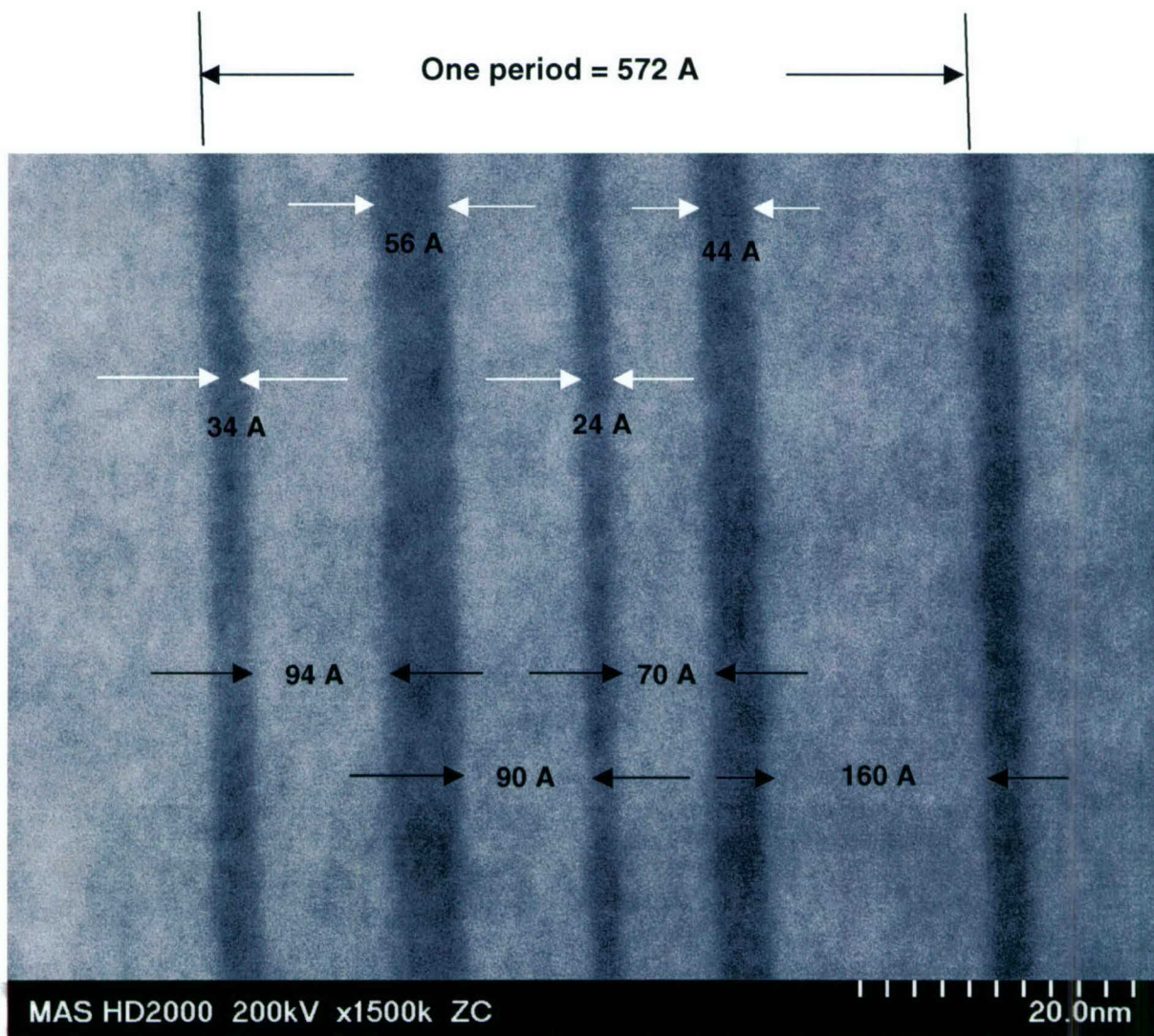
Figure 5 STEM cross-section photograph of Wafer No. M1-1189, section m10, with a scale factor of 2 nm per division (lower right of photo). Dark bands are Al(0.15)Ga(0.85)As, and gray bands are GaAs. Surface of wafer is towards right side of photograph. The layer thickness indicated in black correspond to the layers shown in Table 1 of this report.

Absolute layer thickness calibration in the STEM is difficult, although NIST-traceable standards are available. Spire requested such thickness calibration verification from MAS, and the results are shown in Figure 6.

Comparison of the total layer thickness data obtained from Figure 6 with an NIST standard at MAS suggested a total layer thickness agreement to within better than 1%. Data presented in the following section will confirm this observation.

MAS HD2000 200kV x11.0k ZC   2.00μm

Figure 6   STEM of entire epitaxial growth (Run M1-1189). Because of the reduced magnification it is difficult to pick out the 1200 epitaxial layers in this photograph, but they are there. Comparision to an NIST thickness standard resulted in agreement to better than 1%, an excellent number considering the various potential causes of inaccuracies in absolute dimensional measurements.

2.4   Epitaxial Wafer Growth and Evaluation of the 4 Terahertz Laser Structure

Following successful growth and evaluation of the 3 THz quantum cascade laser structure, growth of the 4 THz structure described in Table 2 of section 2.2 was carried out. This growth (growth run number M1-1280) was carried out approximately 3 months after growth run M1-1189. The results of the STEM cross section analysis of this wafer, as shown in the next few figures, indicate excellent MOCVD growth system reproducibility, testifying to the fact that the MOCVD technology can provide epitaxial THz quantum cascade laser material in production quantities, with excellent quality. Spire's Emcore LDM300 production epitaxial growth reactor has demonstrated monolayer abruptness in transitions between AlGaAs and GaAs epitaxial layers.

Figure 7 is an STEM cross section photograph of wafer M1-1280 with a linear scale of 20 nm, corresponding to 2 nm per small division. This figure shows just a bit more than one period of the structure.

```
MAS HD2000  200kV  x1500k  ZC                                    20.0nm
```
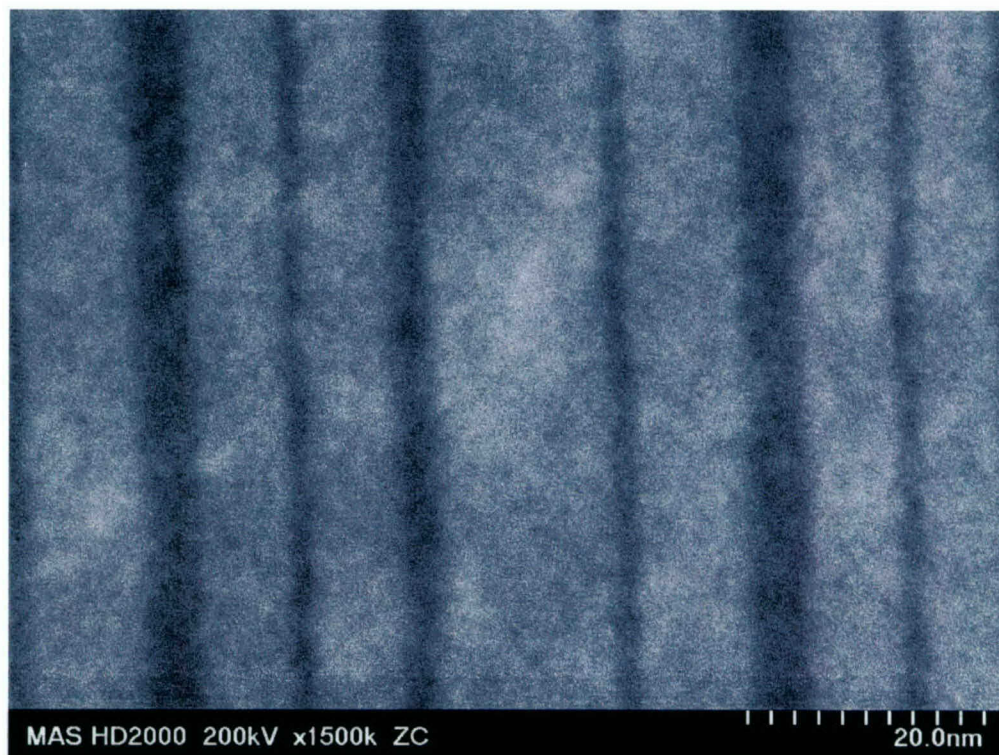
Figure 7   **STEM cross section photograph of a portion of a 4 THz cascade laser wafer from growth run M1-1280. Reference to Table 2 indicates that the thinnest AlGaAs line corresponds to a layer thickness of 22 angstroms, in close agreement with the indicated scale factor. High precision agreement for thickness values can only be obtained by examination of a much thicker portion of the structure.**

From this figure it can be seen that there is excellent agreement in epi-layer thickness values with the epitaxial structure design shown in Table 2 of this report. A somewhat lower magnification cross-section STEM photograph (200 nm scale factor) is shown in Figure 8.

This STEM photograph illustrates the high epitaxial layer thickness uniformity achieved on the Spire Emcore LDM300 production growth system. Recent epitaxial growth of different epitaxial structures with layers as thin as 6 angstroms (2 atomic layers) indicated the same type of uniformity and layer transition abruptness as evident in Figure 8.

2.5   Terahertz Cascade Laser Structure Design

Under subcontract to Spire on this program, the UIUC group developed a theoretical model to simulate surface plasmon waveguides for terahertz quantum cascade (QC) lasers emitting 3 and 4 THz radiation.   The epitaxial layer structures of these lasers are presented in the prior sections of this report. In this analysis, UIUC focused on the most sophisticated types of surface plasmon waveguides: metal-semiconductor-doped semiconductor (MSDS) and metal-semiconductor-metal (MSM) double-sided surface plasmon designs.

MAS HD2000 200kV ×100k ZC   300nm
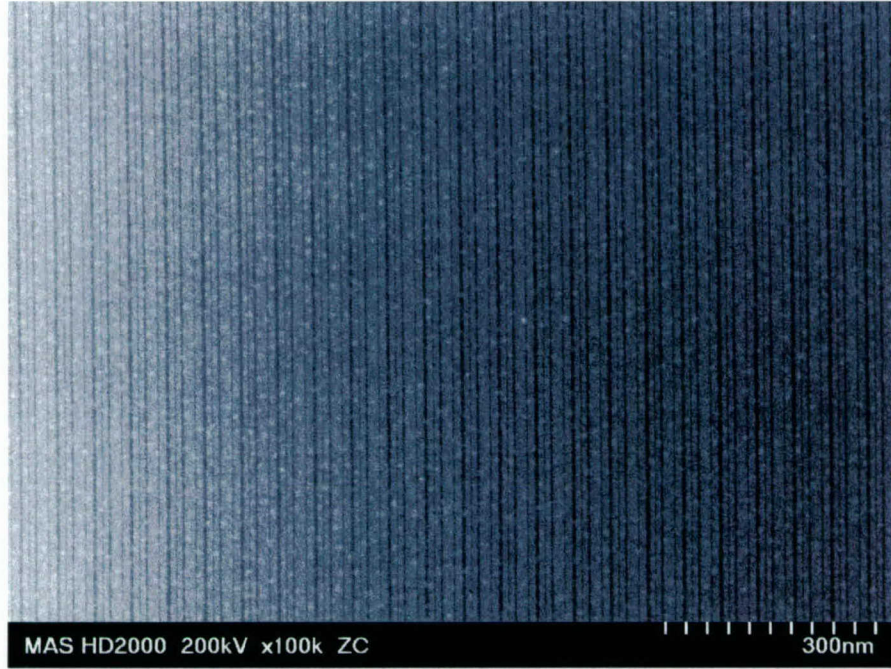
Figure 8   STEM cross-section photograph of wafer M1-1280 showing approx. 24 periods of the 150 period epitaxial structure of Table 2. The excellent uniformity, linearity, and contrast indicate high quality epitaxial crystal growth in Spire's Emcore LDM300 production reactor.

Maxwell equations were solved with appropriate boundary conditions for the transverse magnetic (TM) mode of THz radiation by applying optical transfer matrix formalism. Special cares were taken to find the correct complex propagation constant to ensure the decaying of the fields in the outermost regions. Contour plots were used to help input an initial guess into the "FindRoot" function in order to search for the complex propagation constant. The permittivity of the metal and the doped semiconductor can be calculated using the Drude model where

$$\varepsilon = \varepsilon_o \varepsilon_b \left(1 - \frac{\omega_p^2}{\omega^2 + i\omega/\tau} \right) \text{ and } \omega_p = \sqrt{\frac{ne^2}{\varepsilon_o \varepsilon_b m^*}}.$$ The parameters and values used are summarized

in Table 3.

Table 3   Material parameters used in our simulation, where ε_0= 8.8542x10^{-12}F/m and m_0=9.1x10^{31}kg

Parameter	GaAs (top cladding)	GaAs (Bottom Cladding)	Au
ε_b	12.4	12.4	8
m*	0.067 m$_o$	0.067 m$_o$	m$_o$
n (carrier density)	5x10^{18} cm^{-3}	3x10^{18} cm^{-3}	5.9x10^{22} cm^{-3}

The refractive index of Al$_x$Ga$_{1-x}$As was interpolated at low temperature from the refractive indices of AlAs and GaAs at low temperature which are 2.96 and 3.517 (Ref. 4). The mobility relaxation time constant is related to the Hall mobility. For the n-doped GaAs, the mobility is ~2000 and 2800 cm^2/Vs for the concentration of 4x10^{18} cm^{-3} and 1.8x10^{18} cm^{-3} (Ref. 5) which can be translated into time constants of 106 and 76 fs. In these calculations, the time constants for the doped GaAs layers were interpolated from these values.

10

The simulation results for the 3 and 4 THz QC lasers are broken into four cases as follows:

Case 1) The original design structures. In the preliminary designs, UIUC concentrated on designing multiple quantum well structures to achieve 3 and 4 THz radiation. The mode intensity profiles for 3 and 4 THz waveguide structure are shown Fig. 9(a) and 1(b). There are leakages of the TM field into the substrate, which reduce the optical confinement factor (Γ) of the structure. From these simulation, the Γ for these original structures are 0.21 for 3 THz and 0.33 for 4 THz and the waveguide losses (α_w) are 8.95 cm^{-1} for 3 THz and 9.20 cm^{-1} for 4 THz.
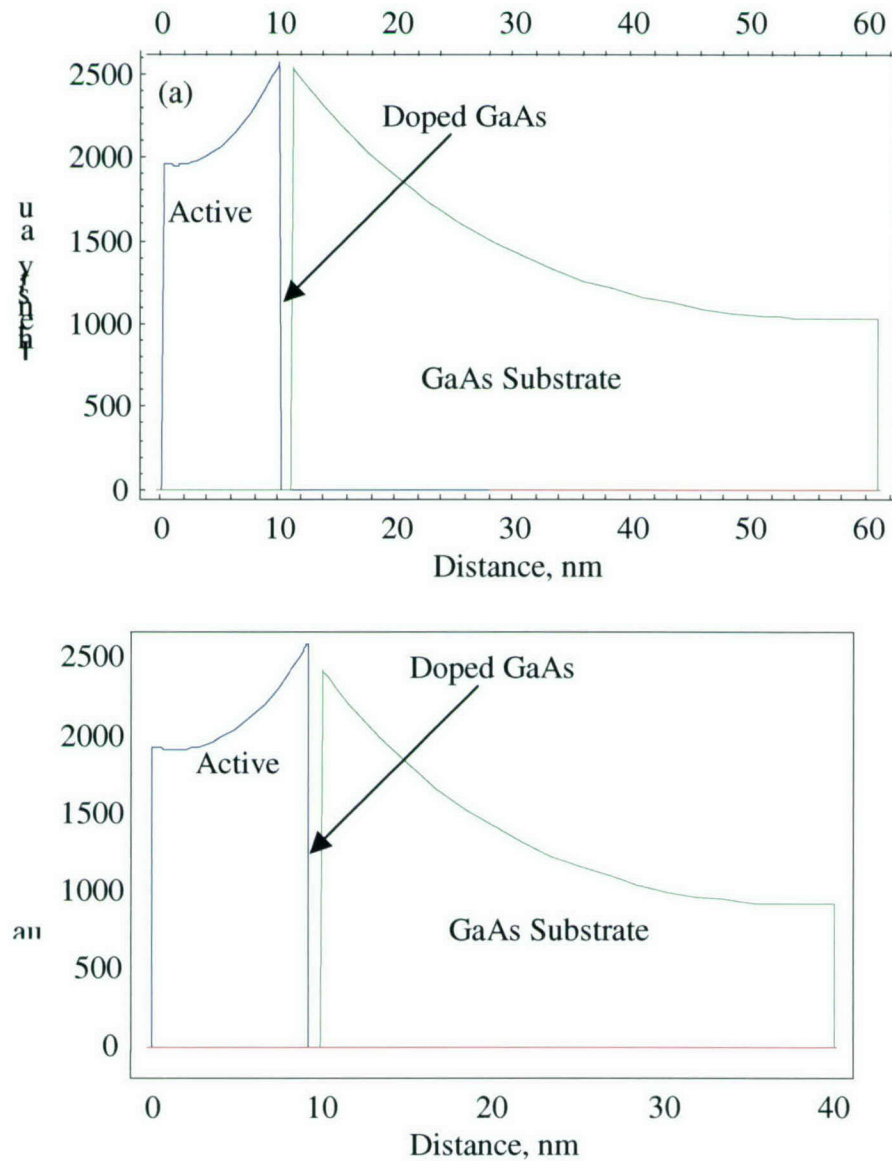
Figure 9 Mode intensity profile for (a) 3 THz design with 175 cascading periods. Γ = 0.21 and the waveguide propagation loss (α_w) is 8.95 cm^{-1}. (b) 4 THz QC design with 175 cascading periods. Γ = 0.33 and the waveguide loss is 9.20 cm^{-1}.

11

Case 2) Since the original sample received from Spire consisted of 150 stages of the active region, it was decided to examine whether or not the structures have a better Γ and α_w than the designs with 175 stages. The mode intensity profile for both 3 and 4 THz are shown in Fig. 10(a) and 2(b).

From the simulation, the optical confinement factor and the waveguide loss are $\Gamma = 0.20$ and $\alpha_w = 8.19$ cm^{-1} for the 3 THz design, and $\Gamma = 0.30$, $\alpha_w = 8.98$ cm^{-1} for the 4 THz design.
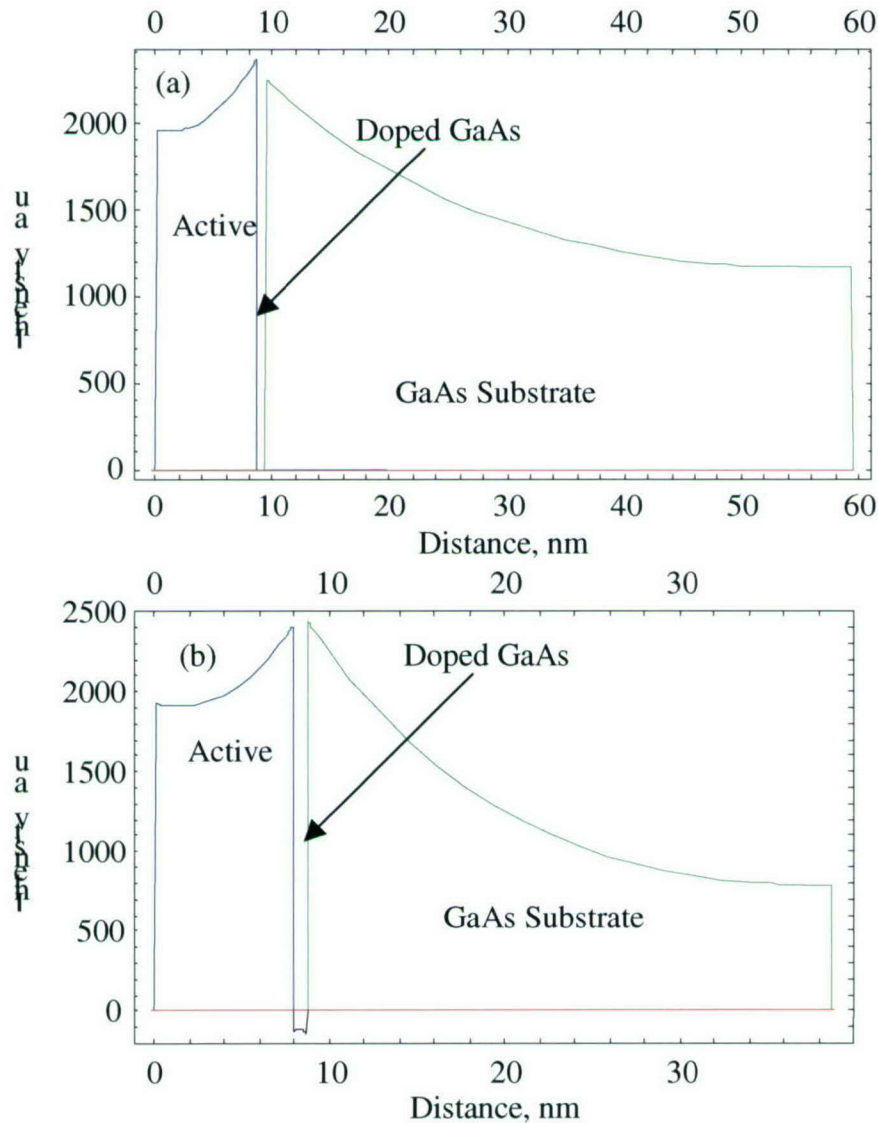
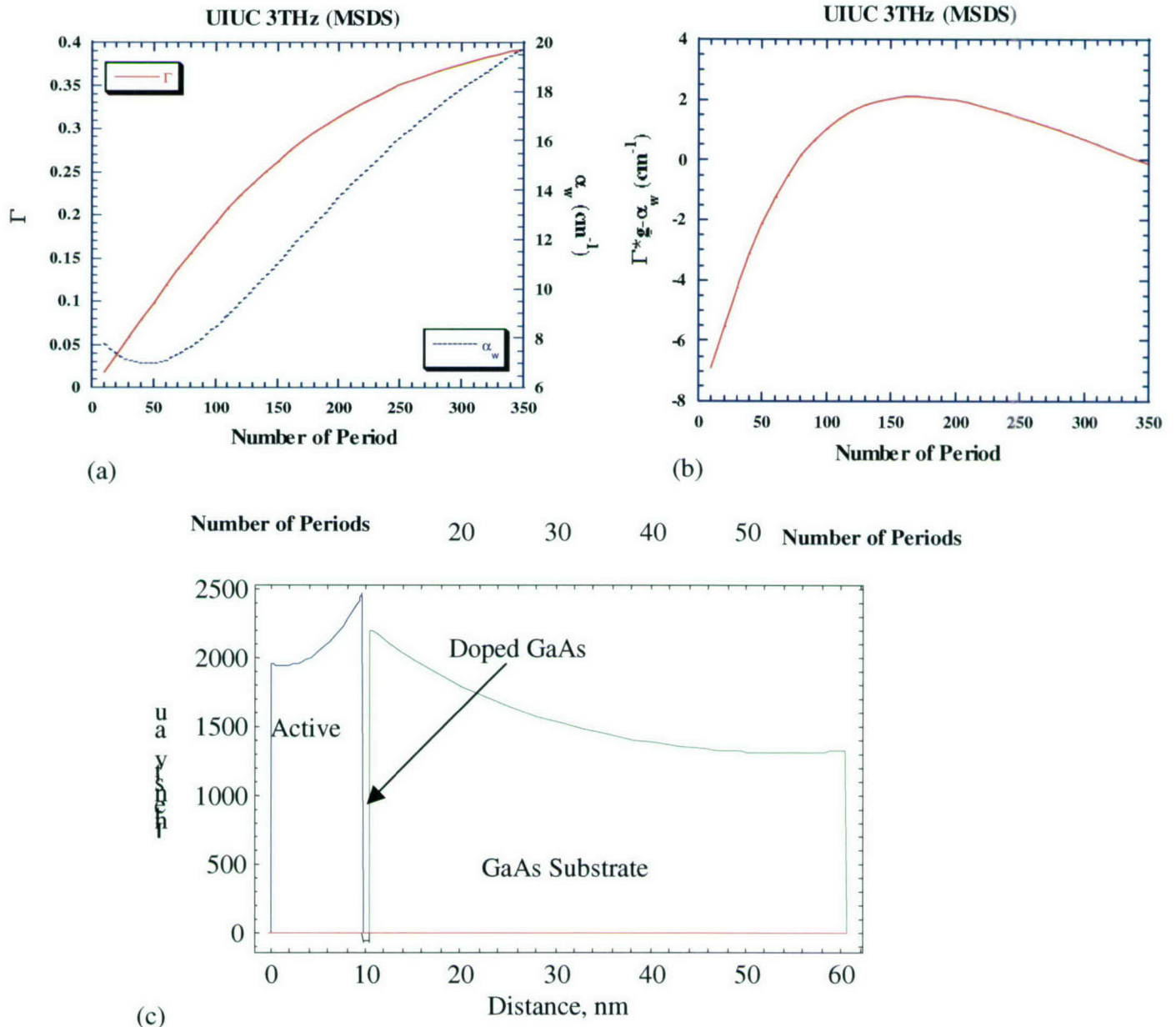Figure 10 Mode intensity profile of waveguides for (a) 3 THz and (b) 4 THz QC lasers with 150 cascading periods.   The optical confinement factor and the waveguide loss are $\Gamma = 0.20$ and $\alpha_w = 8.19$ cm^{-1} for the 3 THz design, and $\Gamma = 0.30$, $\alpha_w = 8.98$ cm^{-1} for the 4 THz design.

12

3) This case is intended to determine the optimum number of the cascading stages to achieve highest possible net gain, $\Gamma*g-\alpha_w$, where g, the material gain per one cascading period and has a value of 50 cm^{-1} from the simulation. For the 3 THz design, 168 stages yield $\Gamma = 0.28$ and $\alpha_w = 12.04$ cm^{-1} with a net gain of 2.104 cm^{-1}, which is better than the result reported in Ref. 9 with $\Gamma = 0.127$ and $\alpha_w = 2.7$ cm^{-1}. A range of 140-170 periods seem to give similar net modal gain of about 2 cm^{-1}. For the 4 THz design, 265 seems to be the optimum number of stages with the optical confinement factor of 0.38 and the waveguide loss of 10.37 cm^{-1} with a net gain of 8.67 cm^{-1}. However, 150 periods give already a net modal gain of 7 cm^{-1}. The results are shown in Figures 11 and 12.

Figure 11 (a) A plot of optical confinement factor and waveguide loss as functions of the number of cascading periods. (b) A plot of net gain, $\Gamma*g-\alpha_w$, as a function of the number of cascading periods. (c) The mode intensity profile of the optimized waveguide (N=168periods). The contacts are metals at the two end positions 0 and around 60 μm.
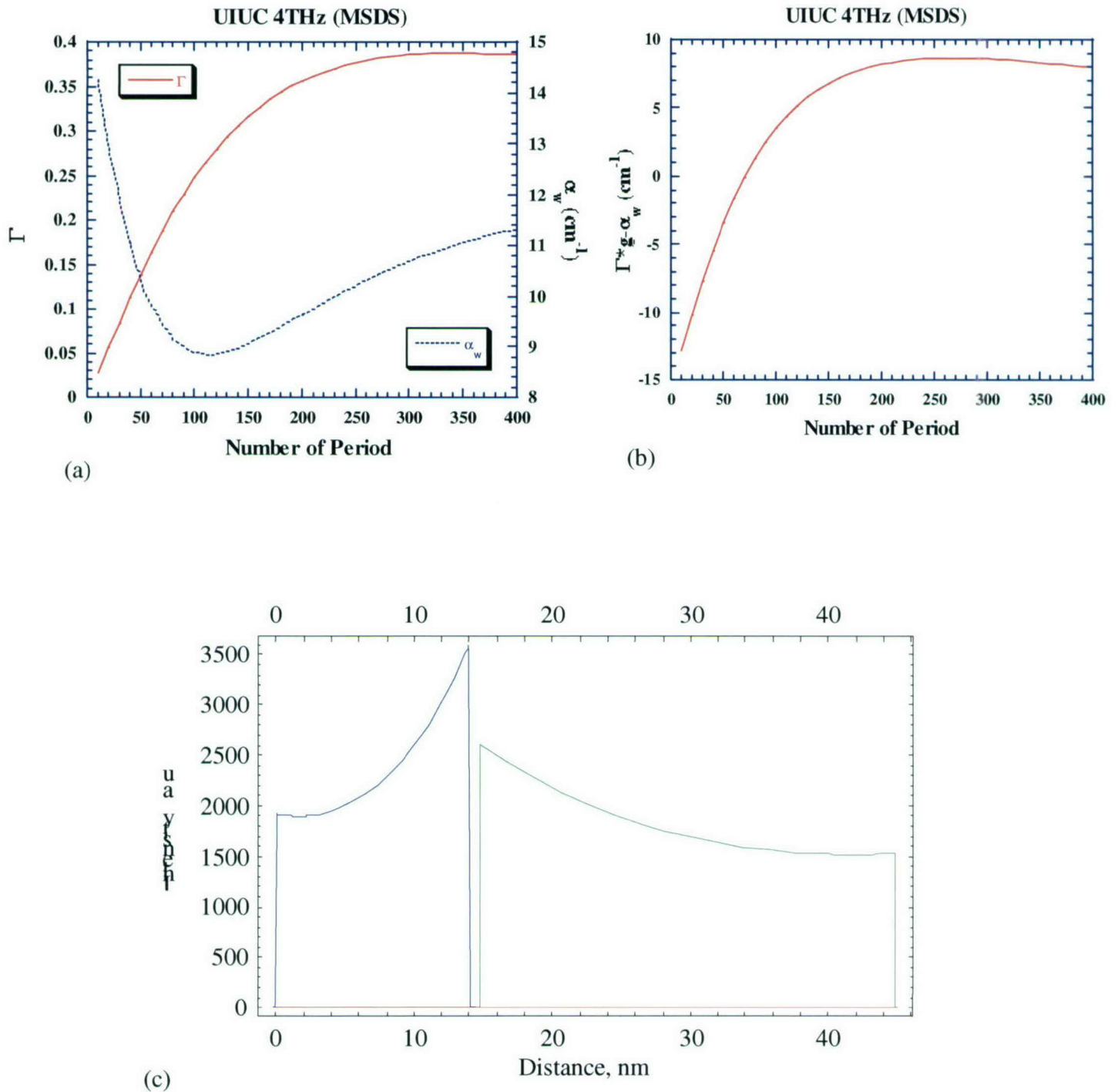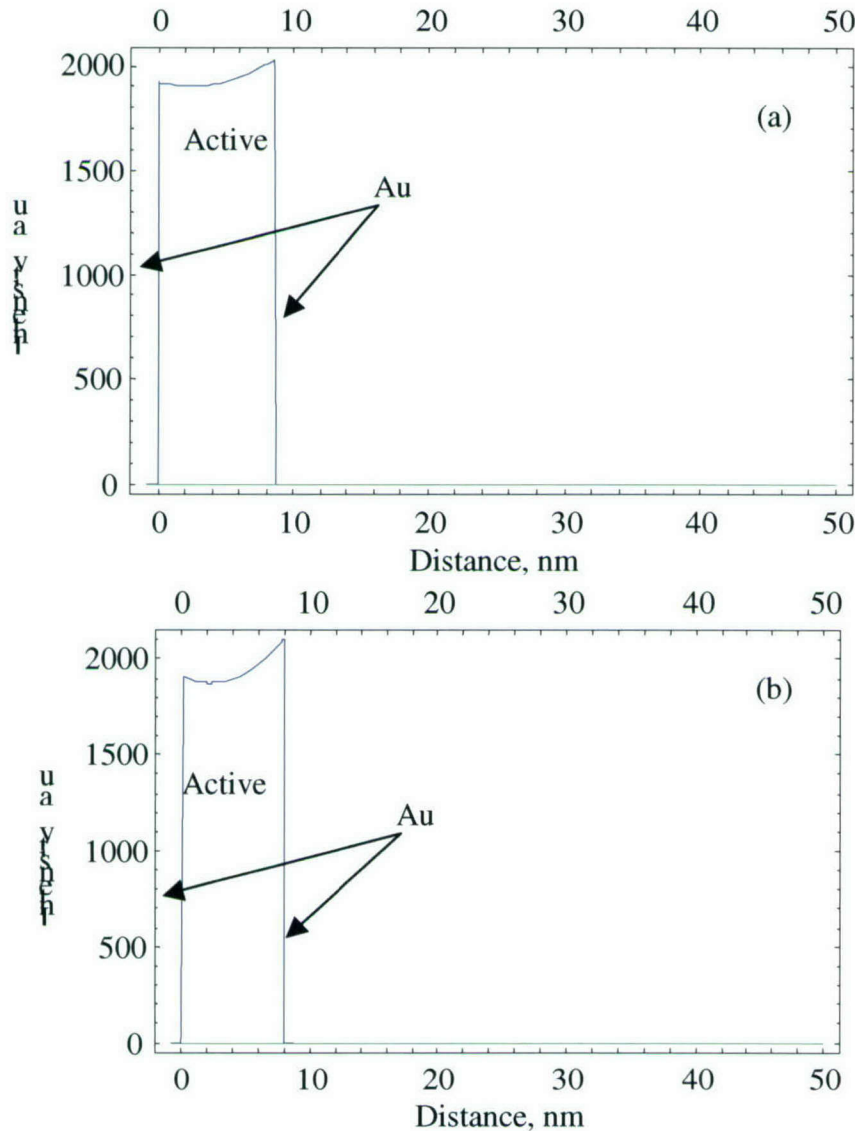
13

Figure 12 (a) A plot of optical confinement factor and waveguide loss as functions of the number of cascading periods. (b) A plot of net gain, $\Gamma^*g-\alpha_w$, as a function of the number of cascading periods. (c) The mode intensity profile of the optimized waveguide (N=265 periods). The top of the active layer (z=0 um) and the bottom of the GaAs substrate (z=45um) are metals.

14

Case 4) The metal-semiconductor-metal (MSM) waveguide structure was investigated for the structures with 150 periods. The optical confinement factor was much better than the metal-semiconductor-doped semiconductor (MSDS) cases with $\Gamma=0.9992$ and waveguide loss of 32.13 cm^{-1} for 3 THz QC lasers. For 4 THz QC laser design, the optical confinement factor was found to have a value of $\Gamma=0.9983$ and waveguide loss of 22.91 cm^{-1}. Whereas this structure yielded better results than the MSDS structure, its attainment requires more processing. The results of the calculations for this structure are presented in Figure 13.

Figure 13 The mode intensity profile of a metal-semiconductor-metal structure for 3 THz (a) and 4 THz (b) QC lasers.

It is important to know the dependence of optical confinement factor, waveguide loss, and net gain on the number of cascading periods for both 3 and 4 THz. From the plots of these parameters as a function of the number of cascading periods, as shown in Figure 14, the confinement factor and net gain increase while the waveguide loss decreases with the number of the periods.

15

Figure 14 (a) A plot of optical confinement factor and waveguide loss as functions of the number of cascading periods for 3 THz. (b) A plot of net gain, Γ*g-α$_w$, as a function of the number of cascading periods for 3 THz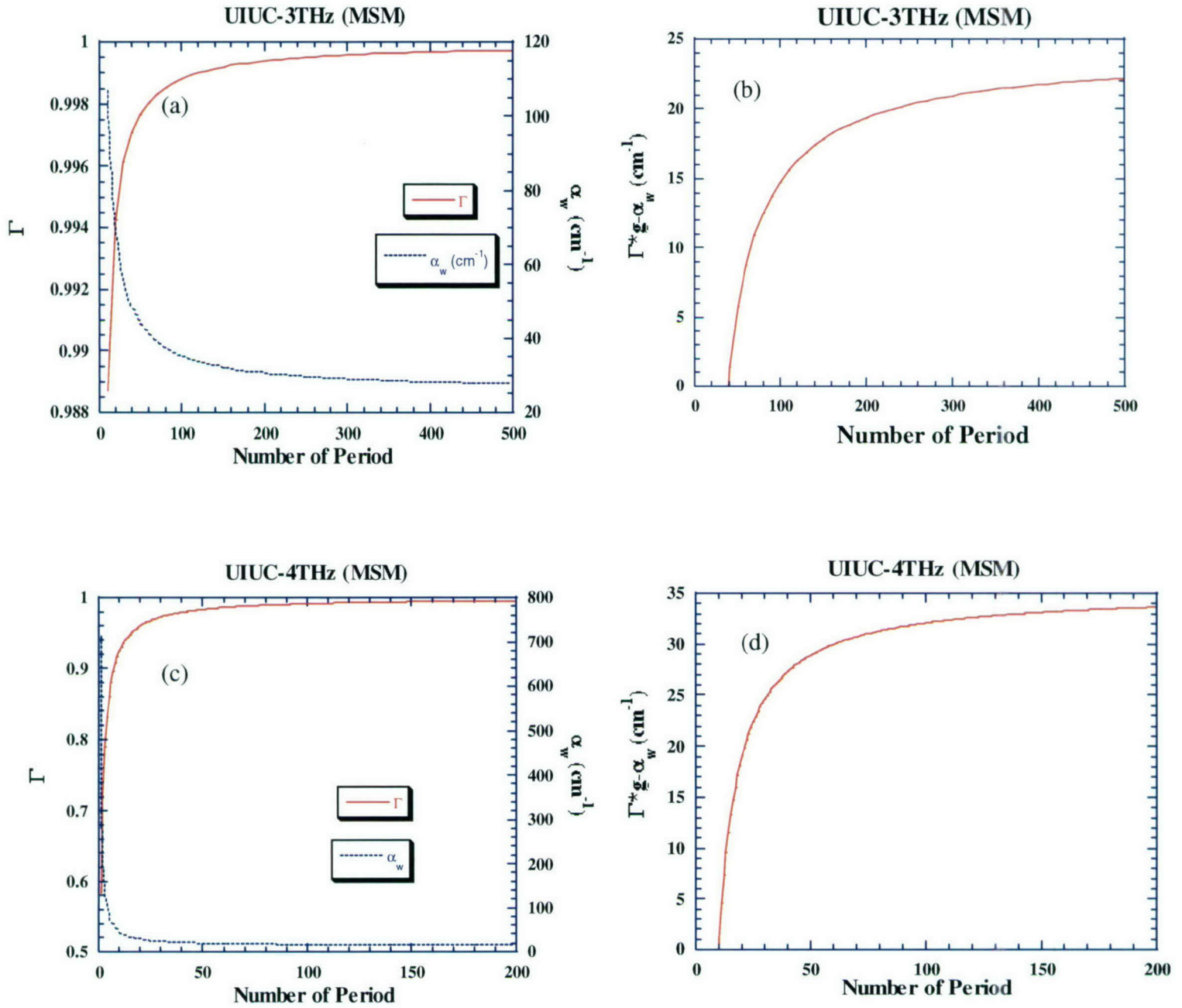. (c) A plot of optical confinement factor and waveguide loss as functions of the number of cascading periods for 4 THz. (d) A plot of net gain, Γ*g-α$_w$, as a function of the number of cascading periods for 4 THz.

In summary, the MSDS waveguide structures have been simulated with different numbers of cascading periods, and only small differences in waveguide quality were found between the UIUC original design and the Spire-grown wafer, $\Gamma = 0.21$ (Case 1a) vs. 0.20 (Case 2a) for 3 THz and $\Gamma = 0.33$ (Case 1b) vs. 0.30 (Case 2b) for 4 THz. These structures are also comparable to the optimized structures with more layers (168 periods for 3 THz and 265 periods for 4 THz). Also, 140-170 periods [Net modal gain is around 2 cm-1, Fig. 3(b)] for 3THz and 150-200 periods [Net modal gain is around 7 to 8 cm-1, Fig. 4(b)] for 4THz designs are acceptable for the MSDS waveguides.

The MSM structures yield far better results than the MSDS structures in terms of optical confinement factor and net gain. MSM structures, though requiring more processing steps, appear to be a better choice. The designs using 150 periods for both 3 and 4 THz should be acceptable.

3. RECOMMENDATIONS FOR THE PHASE II PROGRAM

Based on the results summarized in this Phase I final report, the following tasks are indicated for Phase II:

- Growth of epitaxial wafers using the Spire Emcore LDM300 MOCVD epitaxial deposition system should continue, with epitaxial structures designs generated by the UIUC group. These designs will be modified and optimized in a series of iterations, as cascade laser performance results are obtained.
- The primary cascade laser device structures should be based on the MSM design, although some MSDS designs should also be processed for attainment of comparative device performance results
- Wafer processing should be carried out at Spire, utilizing the state-of-the-art Bandwidth Semiconductor foundry, which has the capability of producing high quality processed epitaxial wafers in ridge-waveguide configurations.
- Quantum cascade laser devices should be fabricated from these wafers, and evaluated for electrical and optical characteristics, including output power, variation of power with drive current, emission spectra, and laser tenability.
- All tasks should be performed in an iterative manner, utilizing design and performance improvements as guides for further device optimization. The primary goal should be to obtain the highest possible cascade laser operating temperatures (with room temperature or above as a goal), and the highest possible output power levels.

4. SUMMARY AND CONCLUSIONS

During this Phase I STTR program, 3 THz and 4 THz quantum cascade laser epitaxial structures were designed and grown by the MOCVD epitaxial growth technology using a commercial MOCVD deposition system. STEM analyses of the wafers grown with these two structures confirmed conformance to design specifications, with epitaxial layer thickness reproducibility to within better than 0.16% when grown several months apart in time. The Spire LDM300 MOCVD epitaxial deposition system used for this work demonstrated outstanding epitaxial material quality and layer uniformity across the multiple wafers grown per run. Laser geometry design studies were carried out using optical electromagnetic field calculations, and it was found that metal-semiconductor-metal (MSM) optical waveguide structures gave considerably better optical confinement than corresponding metal-semiconductor-semiconductor

(MSDS) waveguide structures. Generation of the appropriate computer models, and completion of these preliminary design studies carried out during Phase I makes it possible to produce operational quantum cascade laser devices during Phase II.

5.   REFERENCES

1.   S. L. Chuang, *Physics of Optoelectronic Devices*, (New York: Wiley, 1995).

2.   B. S. Williams, H. Callebaut, S. Kumar, Q. Hu, and J. L. Reno, *Appl. Phys. Lett.*, **82**, 1015 (2003).

3.   S. C. Lee and A. Waker, *Appl. Phys. Lett.*, **83**, 2506 (2003).

4.   F. Yang, J. R. Sambles, and G. W. Gradberry, *Phys. Rev. B.*, **44**, 5855 (1991)

5.   R. Sachs, and H. G. Roskos, *Optics Express*, **12**, 2062 (2004)

6.   S. L. Chuang, *Physics of Optoelectronic Devices*, (New York: Wiley, 1995)

7.   B. Sermage, S. Long, I. Abram, J. Y. Marzin, J. Bloch, R. Planel, and V. Thierry-Mieg, *Phys. Rev. B*, **53**, 16517 (1996)

8.   M. J. Lovejoy, M. R. Melloch, and M. S. Lundstrom, *Appl. Phys. Lett.*, **67**, 1101 (1995)

9.   B. S. Williams, S. Kumar, H. Callebaut, and Q. Hu, *Appl. Phys. Lett.*, **83**, 2124 (2003)